From Drought to Flood: A Water Balance Analysis of the Tuolumne River Basin During Extreme Conditions (2015–2017)

Andrew R. Hedrick
Boise State University

Danny Marks
USDA-ARS Northwest Watershed Research Center

Hans-Peter Marshall
Boise State University

James McNamara
Boise State University

Scott Havens
USDA-ARS Northwest Watershed Research Center

See next page for additional authors

Authors

Andrew R. Hedrick, Danny Marks, Hans-Peter Marshall, James McNamara, Scott Havens, and Ernesto Trujillo

RESEARCH ARTICLE

WILEY

From drought to flood: A water balance analysis of the Tuolumne River basin during extreme conditions (2015–2017)

Andrew R. Hedrick[1,2] | Danny Marks[1] | Hans-Peter Marshall[2,3] |
James McNamara[4] | Scott Havens[1] | Ernesto Trujillo[1,5] | Micah Sandusky[1] |
Mark Robertson[1] | Micah Johnson[1,5] | Kat J. Bormann[6] | Thomas H. Painter[7]

[1]USDA-ARS Northwest Watershed Research Center, Boise, Idaho

[2]Cryosphere Geophysics And Remote Sensing, Department of Geosciences, Boise State University, Boise, Idaho

[3]U.S. Army Cold Regions Research and Engineering Laboratory, Hanover, New Hampshire

[4]Department of Geosciences, Boise State University, Boise, Idaho

[5]Sierra Nevada Research Institute, University of California, Merced, California

[6]Jet Propulsion Laboratory/California Institute of Technology, Pasadena, California

[7]Joint Institute for Regional Earth System Science and Engineering, UCLA, Los Angeles, California

Correspondence

Andrew R. Hedrick, USDA-ARS Northwest Watershed Research Center, Boise, Idaho, USA.
Email: andrew.hedrick@usda.gov

Funding information

Agricultural Research Service, Grant/Award Number: 2052-13610-012-00D; National Aeronautics and Space Administration; California Institute of Technology; NASA Applied Sciences Western Water Applications Office; California Department of Water Resources; NRCS Water and Climate Center, Bureau of Reclamation Pacific Northwest Region; USGS/Earth Resources Observation and Science (EROS) Center; NASA EOSDIS Land Processes Distributed Active Archive Center (LPDAAC)

Abstract

The degree to which the hydrologic water balance in a snow-dominated headwater catchment is affected by annual climate variations is difficult to quantify, primarily due to uncertainties in measuring precipitation inputs and evapotranspiration (ET) losses. Over a recent three-year period, the snowpack in California's Sierra Nevada fluctuated from the lightest in recorded history (2015) to historically heaviest (2017), with a relatively average year in between (2016). This large dynamic range in climatic conditions presents a unique opportunity to investigate correlations between annual water availability and runoff in a snow-dominated catchment. Here, we estimate ET using a water balance approach where the water inputs to the system are spatially constrained using a combination of remote sensing, physically based modelling, and in-situ observations. For all 3 years of this study, the NASA Airborne Snow Observatory (ASO) combined periodic high-resolution snow depths from airborne Lidar with snow density estimates from an energy and mass balance model to produce spatial estimates of snow water equivalent over the Tuolumne headwater catchment at 50-m resolution. Using observed reservoir inflow at the basin outlet and the well-quantified snowmelt model results that benefit from periodic ASO snow depth updates, we estimate annual ET, runoff efficiency (RE), and the associated uncertainty across these three dissimilar water years. Throughout the study period, estimated annual ET magnitudes remained steady (222 mm in 2015, 151 mm in 2016, and 299 mm in 2017) relative to the large differences in basin input precipitation (547 mm in 2015, 1,060 mm in 2016, and 2,211 mm in 2017). These values compare well with independent satellite-derived ET estimates and previously published studies in this basin. Results reveal that ET in the Tuolumne does not scale linearly with the amount of available water to the basin, and that RE primarily depends on total annual snowfall proportion of precipitation.

KEYWORDS

data assimilation, evapotranspiration, headwater catchment hydrology, Lidar, snow modelling, spatial variability, water balance, water resources

1 | INTRODUCTION

A major scientific question in mountain hydrology is how decreasing snowpack and inter annual climate variability will affect runoff ratios and stream flow. Future climate projections for the Western United States overwhelmingly agree that future temperatures will continue to rise (Garfin et al., 2018; May et al., 2018), but future shifts in precipitation are much more uncertain (Luce et al., 2016; Roderick, Sun, Lim, & Farquhar, 2014). Regardless of future precipitation trends, global mountain snow cover duration is shortening (Kunkel et al., 2016), and the likelihood of extreme climatological events is increasing (Jentsch, Kreyling, & Beierkuhnlein, 2007; Seager, Naik, & Vogel, 2012).

One way to investigate the effect of future predictions of climate variability on the water cycle in mountain environments is to disaggregate the hydrologic water balance into its constituent components, which has been the focus of some recent studies. Berghuijs, Woods, and Hrachowitz (2014) used a data-driven approach to infer that basins receiving a higher proportion of annual precipitation as snow experience higher long-term mean stream flow than those basins that are more rain-dominated. Godsey, Kirchner, and Tague (2014) examined measured runoff and snow water equivalent (SWE) across multiple basins in the California Sierra Nevada and found that summer low flows vary proportionately with annual variations in peak SWE. More recently, Cooper et al. (2018) took the investigation of low flow sensitivity one step further by including all winter precipitation and potential evapotranspiration (PET), in addition to SWE, across 110 ungauged basins in the western United States. Their analysis determined that summer evaporative demand is the dominant contributor affecting low flow sensitivity to climate variability. However, low flow sensitivity was found to be tempered in catchments with higher snow proportions of total precipitation, such as is found in the high alpine.

By constraining one or more of the terms of the water balance equation with better measurements and monitoring techniques, the trends in the more poorly understood terms can be estimated with greater accuracy. This process-driven approach for closing the water balance has been shown to be useful for assessing energy and mass balance components that are difficult to measure such as evapotranspiration (ET) (Wan et al., 2015; Williams et al., 2012), groundwater recharge (Henn et al., 2018; Herrmann, Keller, Kunkel, Vereecken, & Wendland, 2015; Kendy et al., 2003), and runoff efficiency (RE) (Knowles et al., 2015), the latter of which is defined as the ratio of basin discharge to precipitation.

Water balance studies assessing basin-wide evaporation and sublimation losses in catchments where more than 80% of annual precipitation falls as snow are uncommon but not unprecedented. Leydecker and Melack (2000) used a complimentary relationship model to estimate aerial ET over various alpine catchments throughout the Sierra Nevada. They found that ET was typically low throughout the months of snow cover, and then markedly increased during the late summer and early autumn of each year with an average of 36% of the water budget lost to the atmosphere. Kattelmann and Elder (1991) examined the water balance of the Emerald Lake watershed in the Southern

Sierra Nevada and found that ET ranged from 19 to 30% of the total water budget in successive years (1986–1987). Henn, Newman, Livneh, Daly, and Lundquist (2018) also found that in the Tuolumne River Basin, the mean late season residual – defined as the combination of ET and groundwater recharge after peak SWE – ranged from 30 to 39% of the annual water budget for three recent drought years (2013–2015).

Following this recent drought (2012–2015), the California Sierra Nevada underwent the largest dynamic range of snowpack conditions over a 3-year period in recorded history (2015–2017). The final year of the drought (2015) resulted in the lowest April 1 snowpack in over 500 years, according to a tree-ring SWE reconstruction study (Belmecheri, Babst, Wahl, Stahle, & Trouet, 2016). The following winter of 2016 resulted in a near-average snowpack, with April 1 SWE totals around 85% of the recorded average. Lastly, the winter of 2017 resulted in the second highest April 1 SWE in recorded history, and the most reservoir inflow on record for many of the large reservoirs along the western slopes of the Sierra Nevada. These three climatically dissimilar years provide a backdrop for examining hydrologic responses across a wide range of conditions.

The primary question this study aims to answer is *how are ET and RE in an alpine/subalpine environment affected by both total water availability and the snow fraction of precipitation entering the basin?* A secondary question is then *to what degree do periodic Lidar snow depths decrease uncertainty in modelled ET and RE estimates?* To investigate these questions, we simulate the snowpack at an hourly time scale over the water years 2015–2017. We use a fully distributed physically based energy and mass balance snow model forced with hourly gridded meteorological fields derived from weather station measurements in 2015 and 2016, and downscaled atmospheric model forecasts in 2017. The snow model is then updated with periodic distributed NASA Airborne Snow Observatory (ASO) snow depths at 3-m resolution covering the entire basin domain, explicitly resolving the spatial distribution of SWE and effectively improving the snow input precipitation estimates over the basin. These updates have been shown to drastically increase the accuracy and reliability of modelled SWE throughout the melt season (Hedrick et al., 2018), as the Lidar depth fields correct for large uncertainties in input snowfall magnitudes and simulated melt rates. Combined with some fundamental assumptions about the hydrologic behaviour of the Tuolumne Basin over an annual time scale we place the resulting estimates of ET and RE in the context of the Budyko relationship (Budyko, 1974) to explain the relationship of RE with annual basin precipitation and snowfall fraction. The water balance approach detailed here provides an additional perspective on how a large snow-dominated headwater catchment responds to climate variability.

2 | STUDY AREA AND MODEL APPLICATION

This study was performed over the Tuolumne River Basin in the Sierra Nevada, California (Figure 1). The outlet of the basin is at the base of O'Shaughnessy Dam (37.947386°N, 119.788497°W), which forms

Hetch Hetchy Reservoir and provides the main source of drinking water and hydropower to nearly 3 million residents in the city and county of San Francisco. The total basin area is 1,187 km² and elevations range from 1,150–3,999 m, with over 90% of the basin lying above 2,000 m, which has been the average approximate rain-snow transition elevation in the basin since 2013 (Hedrick et al., 2018). Elevations between 2,000 and 2,900 m are mainly composed of snow-dominated subalpine forests and make up 55% of the total basin area. The upper 35% of the basin (2,900–3,999 m) is an alpine environment where the snow distribution is heavily influenced by wind. The Tuolumne lithology is composed of mainly intrusive granodiorite bedrock with soils over much of the basin being less than 1-m deep (Lundquist et al., 2016). Numerous hydrologic studies have been performed in the Tuolumne Basin (e.g., Henn, Newman, et al., 2018; Lundquist, Dettinger, & Cayan, 2005; Raleigh & Small, 2017; Rice, Bales, Painter, & Dozier, 2011) owing to its significance and status as a vital "water tower" for downstream inhabitants (Viviroli, Dürr, Messerli, Meybeck, & Weingartner, 2007).

2.1 | *iSnobal* and the airborne snow observatory

This study's approach to examine the water balance of the Tuolumne Basin involves estimating the timing and magnitude of snowmelt and
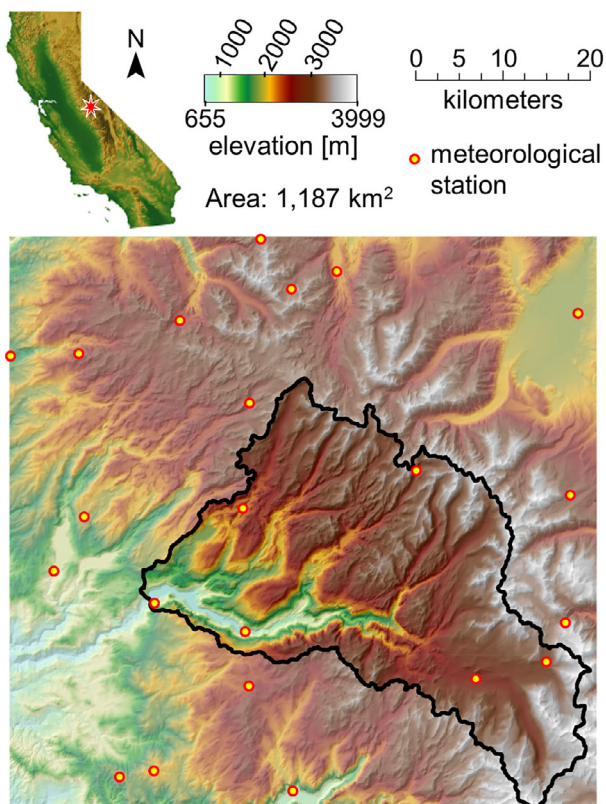

FIGURE 1 Location and relief map of the Tuolumne River Basin above Hetch Hetchy Reservoir within the U.S. State of California. Locations of various measurement stations used to force *iSnobal* in water year 2015 and 2016 are depicted as yellow circles

rainfall entering the hydrologic system using a physically based snow-melt model. The *iSnobal* model (Marks, Domingo, Susong, Link, & Garen, 1999) has been tested extensively across various climate regimes and has been shown to produce reasonable estimates of basin-wide snowpack mass over annual timescales (Hedrick et al., 2018; Kormos et al., 2014; Reba, Marks, Winstral, Link, & Kumar, 2011; Sohrabi et al., 2019; Winstral, Marks, & Gurney, 2013). In this application, *iSnobal* provided daily predictions of various energy and mass fluxes at 50-m spatial resolution for water years 2015–2017. During water years 2015 and 2016, the model was forced using hourly weather station measurements from co-operator sites in and around the basin, interpolated to each model grid cell (Figure 1). These methods are presented in detail by Havens, Marks, Kormos, and Hedrick (2017) and Hedrick et al. (2018). However, the near-record snowfall totals in 2017 buried meteorological instrumentation at multiple sites, and alternatively, downscaled gridded meteorological forecast products from the National Oceanic and Atmospheric Administration's High-Resolution Rapid Refresh (HRRR; Benjamin et al., 2016) operational model were used instead as model forcing inputs. This approach to using atmospheric forecast models as *iSnobal* forcing data was developed and described by Havens et al. (2019).

In addition to the hourly meteorological forcing fields, the model can also be constrained by spatial observations of the snow depth state variable whenever these measurements are available. Since 2013, the NASA/Caltech Jet Propulsion Laboratory ASO has performed airborne Lidar and spectrometer surveys throughout each ablation season to periodically determine the spatial distribution of snow depth (Painter et al., 2016) across the Tuolumne River Basin. These Lidar-derived snow depth measurements provide a more realistic snowpack distribution, which in turn improves snow energy and mass calculations. This improvement ultimately provides more accurate estimates of snowpack thermal state, melt and runoff, which combined with rainfall is here referred to as surface water input (SWI). The procedure for updating *iSnobal* whenever ASO measurements are available is described by Hedrick et al. (2018). The number of ASO model updates varied each year of this study from 9 flights in 2015, 12 flights in 2016, and 8 flights in 2017.

3 | BACKGROUND AND METHODS

The general water balance of a basin over a specified duration can be represented as

$$\Delta S = P + \Delta G - (Q + ET), \tag{1}$$

where ΔS is the difference in water stored within the basin between the beginning and end of the duration (i.e., change in soil moisture), P is the total precipitation input to the basin as rain and snow, ΔG is the difference between incoming and outgoing groundwater across subsurface catchment boundaries, Q is the cumulative basin runoff at the basin outlet, and ET is the combination of water returned to the

atmosphere by evaporation, snow sublimation, and transpiration by vegetation. We use Equation (1) to solve for total annual ET by applying some simplifying assumptions described below.

Owing to the unique lithology of the basin (Lundquist et al., 2016), we assume that cross-basin subsurface water transfers are negligible so that

$$\Delta G \approx 0. \tag{2}$$

Equation 2 implies that all groundwater within the basin originated as precipitation within the catchment area. The change in groundwater and soil storage is also zero if the basin begins and ends the specified duration at the same wetness state, that is, groundwater levels, soil moisture contents, and SWE storage are approximately the same regardless of variations that occurred within the time duration. We begin the water year on October first each year, when the basin tends to be at its driest state, and we assume

$$\Delta S \approx 0. \tag{3}$$

A portion of ET includes a term E_S, which here represents both evaporation and sublimation from the snowpack. Common methods to compute ET do not include snow processes, therefore we introduce a new term ET_{WB}, which is the water balance-derived ET with E_s removed. E_s is modelled within *iSnobal* using air temperature and the latent heats of vaporisation and sublimation (Marks, Kimball, Tingey, & Link, 1998). Once these atmospheric moisture fluxes from the snow surface have been disentangled from P, we then define SWI, referenced in Section 2.1, as any water that strikes the soil as either rain on bare ground, melt water at the snow-soil interface, or rain that percolates through the snowpack. Assuming all snow from the previous year melts before Oct. 1 and that Equations (2) and (3) are approximately true, then

$$SWI = P - E_s, \tag{4}$$

Equation (1) can then be simplified such that

$$ET_{WB} = SWI - Q + \varepsilon, \tag{5}$$

where ET_{WB} is the water balance-derived ET, ε is a residual error term that comprises both measurement uncertainty in P and Q, along with model uncertainty in P, E_S and assumptions regarding ΔS and ΔG. Next, we will explore each variable of this reduced water balance Equation (5) independently in the context of this study.

3.1 | Evapotranspiration

Previous work has estimated ET amounts in the Sierra Nevada using water balance approaches (Henn, Painter, et al., 2018; Kattelmann & Elder, 1991) and regression relationships between eddy covariance flux tower measurements and satellite products (Fellows &

Goulden, 2017; Goulden et al., 2012; Roche, Goulden, & Bales, 2018). These approaches focused on different applications but concluded that annual ET in the upper elevations of the Sierra Nevada ranged between 150 and 400 mm, with most of the losses occurring below tree line. In fact, the regression-based studies estimated ET only as high as the subalpine environment, since the highest elevation flux tower site used to determine the relationship is at 2,700 m. Over 60% of the land area within the Tuolumne Basin is above that elevation and is heavily snow-dominated, shortening the annual duration when ET can occur. Following the elevational trends of ET presented in the literature, the actual total ET in this headwater catchment is likely towards the lower end of previous estimates due to the lack of vegetation in the upper reaches of the basin. This study will estimate ET, along with uncertainties represented in ε, by using measurements of Q and by constraining P and E_s using combined remote sensing and modelling results.

In addition to the flux tower transects, optical satellite products, and water balance approximations, satellite retrieval algorithms can be used as independent validation sources for estimating actual ET. The MOD16 Global Evapotranspiration Product was first described by Mu, Heinsch, Zhao, and Running (2007) and based on algorithms from Cleugh, Leuning, Mu, and Running (2007), with an improved algorithm described by Mu, Zhao, and Running (2011). MOD16 is derived from MODIS-derived land cover type, Leaf Area Index, and albedo, and is used in this study as a comparison data set for estimated ET_{WB}. MOD16 provides estimates of terrestrial ET every 8 days at 500 m spatial resolution. MODIS Tile H08V05 was downloaded from the NASA Land Processes Distributed Active Archive Center for time period of October 1, 2014 to October 1,2017 (Running, Mu, & Zhao, 2017). Screening of clouds and aerosols is already included in the most recent Version 6 products, but we performed further snow cover masking in a post-processing step using the ASO-updated *iSnobal* model product upscaled from 50 to 500 m. We used the snow-free ASO Lidar returns to further characterize the 500 m MODIS pixels as containing vegetation or being vegetation-free. This decision was made because ET is assumed to be negligible over exposed bed rock, which was determined from snow-free Lidar data to comprise approximately 60% of the Tuolumne Basin. The resultant time series of ET losses from the MOD16 algorithm thus contain spatiotemporal gaps in information due to snow cover, highlighting the limitation of using remote sensing products to derive ET in snow-dominated basins. Until that time when satellite retrieval algorithms are able to provide more robust ET estimates over snow, modelling approaches will remain the most viable means for spatial ET estimation in snow-covered regions.

3.2 | Precipitation

Over all three water years in this study, 29 periodic snapshots of Lidar-derived snow depths from ASO have been directly inserted into the *iSnobal* modelling framework to update the depth state variable in near-real time. These updates allow *iSnobal* to more accurately

simulate the energy and mass balance in each pixel, resulting in more accurate estimates of SWI (Hedrick et al., 2018). Since SWI is the result of explicitly solved energy and mass balances, and informed by high-resolution remote sensing measurements, the hydrologic inputs in this study are more spatially representative than other coarser gridded precipitation products. Henn, Newman, et al. (2018) described the difficulty and uncertainty involved in estimating spatially distributed precipitation in mountainous terrain using coarse regional-scale models. Snow accumulates preferentially due to wind and topography at the hillslope scale (Musselman, Pomeroy, Essery, & Leroux, 2015; Pomeroy, Gray, & Landine, 1993; Trujillo, Ramírez, & Elder, 2007, 2009; Winstral et al., 2013), while accumulation at the basin scale is governed by elevational lapse rates (Feld, Cristea, & Lundquist, 2013; Grünewald, Bühler, & Lehning, 2014; Kirchner,
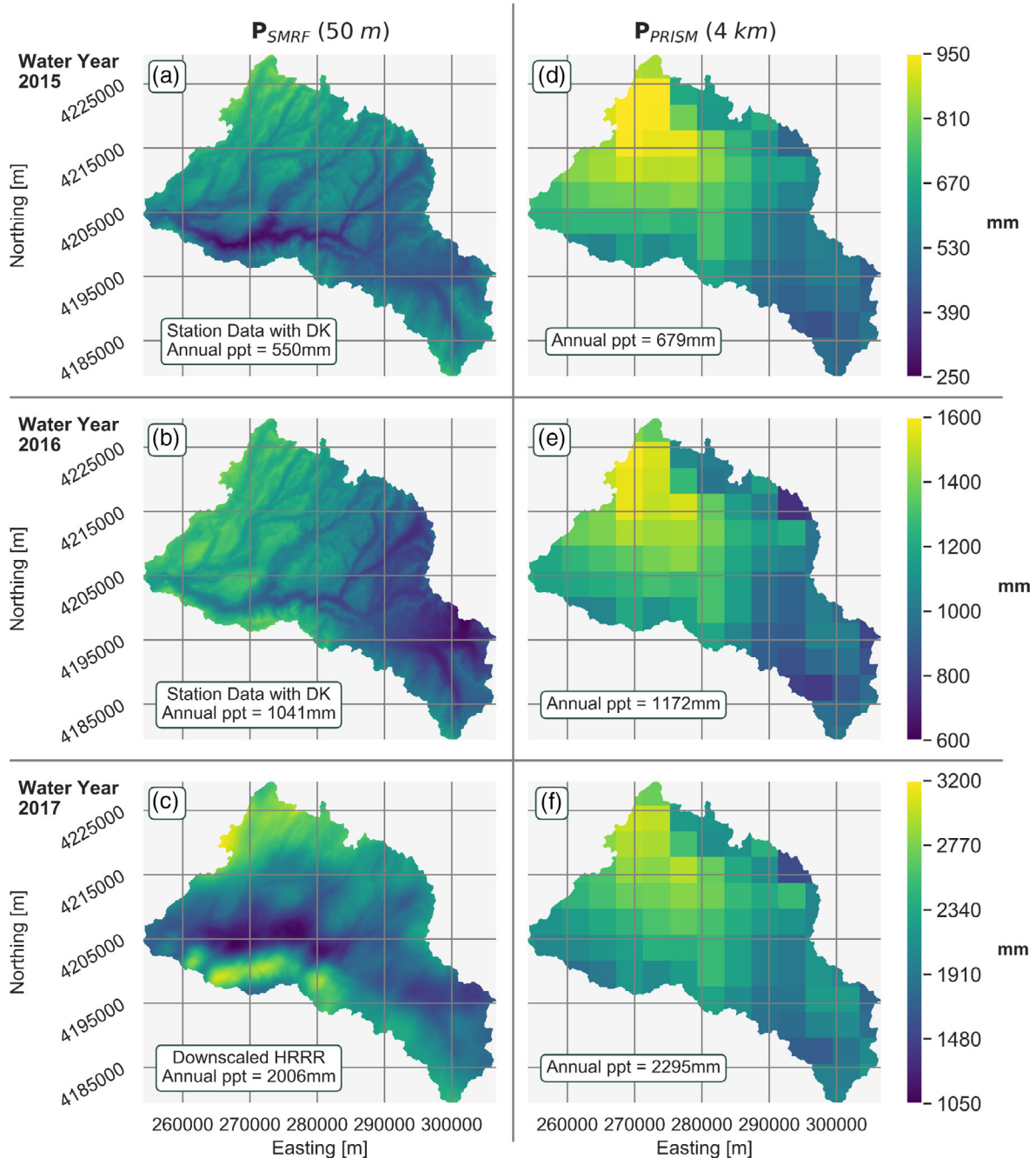

FIGURE 2 Comparison of Spatial Modelling for Resources Framework (SMRF) 50 m and Parameter-elevation Regressions on Independent Slopes Model (PRISM) 4 km cumulative precipitation products over the Tuolumne Basin for water years 2015–2017. Station measurements and detrended kriging produced the SMRF distributions in 2015 and 2016, while 2017 used the downscaled High-Resolution Rapid Refresh forecast due to the higher snowfall amounts and lack of high elevation station measurements. SMRF produces daily precipitation estimates throughout the year, while PRISM is a reanalysis product. Estimates of P_{PRISM} ranged between 13–23% higher than P_{SMRF}

Bales, Molotch, Flanagan, & Guo, 2014; Lehning, Grünewald, & Schirmer, 2011) and orographic effects from atmospheric circulation (Roe & Baker, 2006).

A detrended kriging (DK) technique (Garen, Johnson, & Hanson, 1994) was used to distribute station measured precipitation over the 50-m modelling grid for the drought and average years of 2015 and 2016, respectively. The DK distributing procedure is a submodule of the Spatial Modelling for Resources Framework (SMRF) that was first introduced by Havens et al. (2017). In 2017, when individual storm totals exceeded 400 mm and the annual total topped 2,000 mm, many of the precipitation gauges that had been used in previous years became buried or were significantly capped so as not to be useful. To mitigate this lack of in situ forcing data, gridded precipitation was determined for that year using forecast products from the HRRR model (Benjamin et al., 2016) and an interpolation scheme described by Havens et al. (2019). Subsequently, in all 3 years, regardless of the method used for distributing precipitation, the distribution of snow depth was then updated with the Lidar snow depths whenever an ASO survey took place.

The precipitation distribution routine in SMRF is evaluated by comparing annual cumulative precipitation at 50-m distributed using the DK distribution method (Garen et al., 1994) for 2015–2016, and downscaled using gridded interpolation of the HRRR forecast product for 2017 (Figure 2a,c), to the well-established climate analysis product Parameter-elevation Regressions on Independent Slopes Model (PRISM; Daly, Neilson, & Phillips, 1994) (Figure 2d–f). The DK distributions (Figure 2a,b) are derived from station measurements and can represent both local elevation gradients and large-scale rain shadow effects.

3.3 | Streamflow

The Tuolumne River flows into Hetch Hetchy Reservoir, which is managed by the San Francisco Public Utilities Commission. To understand the water balance of the Tuolumne basin, reconstructed full natural flow (FNF) at the outlet of O'Shaughnessy Dam is used as a proxy for basin discharge. FNF, also referred to as unimpaired runoff, is defined to be the natural discharge that would have occurred without the presence of any dams or diversions upon the stream course. Using daily observed reservoir stage height and measured reservoir releases over the period of record (1970–present), a mass balance approach yields the daily FNF into the reservoir. Lundquist et al. (2016) estimated the uncertainty in the daily reconstructed flows to be on the order of 10%, which is the uncertainty value assigned here to basin discharge (Q). Estimates of cumulative FNF since 1970 and the mean value since 1919 (Figure 3) highlight the large dynamic range of streamflow magnitudes for the 3 years considered here (2015–2017).

3.4 | Snowpack evaporation and sublimation

The amount of atmospheric moisture lost from the snowpack to the atmosphere is a nontrivial portion of the overall water balance and

should not be ignored. Evaporation/condensation of liquid water from/to a surface occurs when the surface's temperature is at or greater than the freezing point ($T_s \geq 0°C$). Conversely, in a snowpack where $T_s \leq 0°C$, ice crystals are able to sublimate into water vapour, resulting in a loss in snowpack mass, and water vapour can condense into frozen ice resulting in mass gain. For a melting snowpack, or $T_s = 0°C$, the atmospheric moisture flux formulation in *iSnobal* is a combination of both sublimation and evaporation, so the magnitude is determined by the overall contribution of the latent heats of vaporisation and sublimation. In the process of computing the latent heat flux term of the snow energy balance, *iSnobal* iteratively solves for the evaporative mass flux, E_S, which is provided as model output. The mathematical representation of the set of nonlinear equations required for computing sublimation and condensation from a snowpack is described by Marks and Dozier (1992) and Marks et al. (2008), and is based on the stability functions found in Brutsaert (1982).

3.5 | Residual (uncertainty term)

The final term of the water balance in Equation (5) is the residual, **ε**, containing the error terms in this particular formulation of ET_{WB}. The error can be subdivided into both measurement and model uncertainty, each of which is considered separately.

The measurement uncertainty is the difference in actual conditions and reported values over the 3 years for P and Q. As mentioned in Section 3.3, a ± 10% uncertainty can be attributed to the reconstructed measurements of Q. Measuring snowfall in mountain environments is often very difficult due to high wind speeds during storms (Rasmussen et al., 2012). Even though the precipitation measurements used in this study are corrected for wind under catch, we have designated a conservative estimate of uncertainty in total basinwide annual P as ±10%. This estimate was essentially assigned as an uncertainty placeholder to demonstrate how error propagates into the water balance results and could be higher or lower in reality. Additionally, no error assessments have yet been conducted on the HRRR precipitation product used in 2017, so we have assigned the same 10% uncertainty value for that water year.

Sources of model uncertainty stem from three main aspects in this study. First, error is introduced by the assumptions made in Equation (2) and Equation (3), because the actual changes in storage and groundwater fluxes on annual time scales may often be nonzero. A recent study used small elevation displacements measured by ground-based Global Positioning System stations to determine annual changes in subsurface water storage throughout the entire Sierra Nevada (Enzminger, Small, & Borsa, 2019). Their findings showed that the subsurface water storage generally decreased during the drought period of 2011–2016, and that large annual increases in storage was well-correlated to large precipitation years like 2017. However, we are not able to make inferences about storage specific to this high elevation snow-dominated basin, since the findings of that study were averaged over the entire Sierra Nevada and included rain-dominated lower elevations. If the aquifer was drawn down during the drought
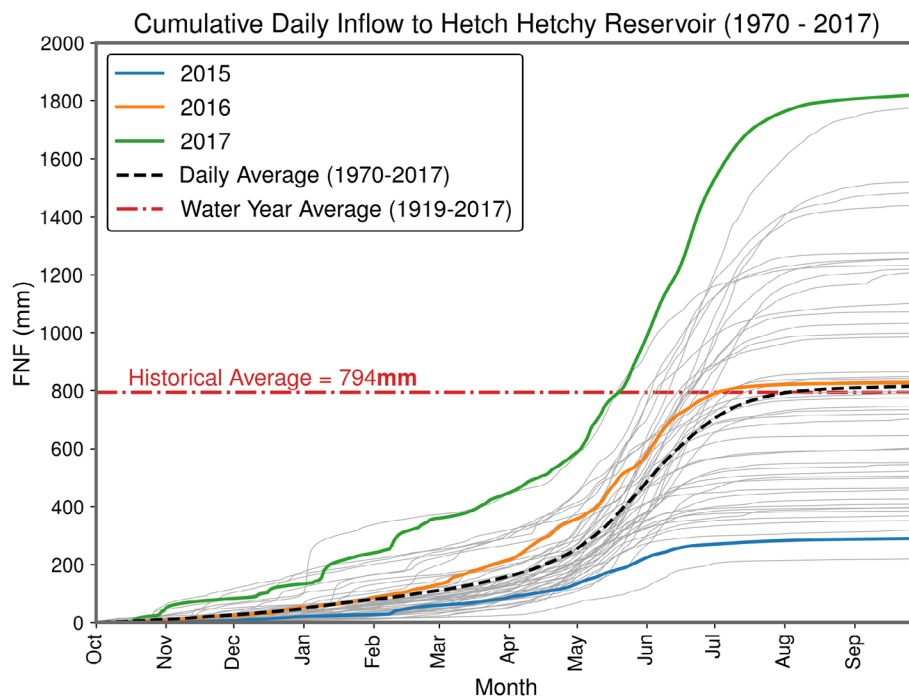
FIGURE 3 Cumulative estimated daily full natural flow into Hetch Hetchy Reservoir showing the relative climatic variability of 2015–2017 from daily measurements that began in 1970. Additionally, from 1919–1970 mean inflow estimates were kept by hand and the mean inflow since the dam construction is shown as the dash-dotted horizontal line

and recharged in 2016 and 2017, as is shown by Enzminger et al. (2019) and other studies (e.g., Bales et al., 2018), then ET_{WB} in those years would be overestimated. We can also look to other available in situ data to test the applicability of the approximation made by Equation (3). The total soil water content from a recent soil moisture dataset (Stern, Anderson, Flint, & Flint, 2018) at two sites in and just outside the basin showed very little variation from one water year to the next. Furthermore, each of the three study years produced some carryover of modelled SWE into the next water year, though these quantities were quite insubstantial (as percentages of cumulative P: 0.0016% for 2015, 0.0275% for 2016, and 0.1151% for 2017).

A second source of model uncertainty is the process of distributing meteorological variables from both point measurements and 3-km gridded forecast products to the 50-m model grid. Lastly, there are inherent model errors in the formulation of the nonlinear differential equations used within *iSnobal* to estimate sensible and latent heat fluxes. For a more simplistic approach, this study assumes that all these model errors are unbiased and normally distributed, for which these errors would by definition sum to zero when integrated over the entire year and basin.

Once measurement and model uncertainties have been considered, a bulk residual value can be estimated by comparing the distributions of ASO measured snow depths with the *iSnobal* modelled snow depths. Previous work has shown that the root-mean square error (RMSE) between modelled and measured snow depths decreased by a factor of three when prior ASO updates had occurred earlier in the season (Figure 6, Hedrick et al., 2018). The trend in RMSE reduction was similar when the entire set of 29 ASO surveys from 2015–2017 was examined. Therefore, barring uncertainties in the energy balance formulation in *iSnobal*, the estimated uncertainty in estimated P, and

subsequently SWI and E_S, is decreased threefold from ≈10 to ≈3% when the ASO updates are used to resolve the snowpack distribution.

4 | RESULTS AND DISCUSSION

Accurate estimates of precipitation, as the lone input term to the hydrologic system, are essential for closing the water balance of the Tuolumne. The downscaled HRRR precipitation in 2017 (Figure 2c) continues to display the northwest to southeast gradient in precipitation present in the DK distributions, but also results in what appear to be localized artefacts of higher precipitation in the southern portion of the basin. These artefacts most probably result from the dynamical downscaling of global climate models and data assimilation routines used within HRRR. Regardless of the source of precipitation estimate, the SMRF precipitation (P_{SMRF}) is produced in near-real time as the water year progresses, in order to provide up-to-date hydrologic conditions to reservoir managers downstream. On the other hand, the PRISM product (P_{PRISM}) is only available a few months after the conclusion of each water year and therefore is not suitable to be used for real time hydrologic prediction. Within the Tuolumne Basin, P_{PRISM} was greater than P_{SMRF} in all 3 years, yet the spatial structure of where precipitation falls is more topographically defined by P_{SMRF} (Figure 2). Further analysis is needed to determine the absolute accuracy of either precipitation product, but this comparison shows that even in the absence of ASO snow depth measurements the forcing precipitation used for *iSnobal* is a reasonable initial step towards accurately simulating the snowpack accumulation.

The ASO snow depth updates throughout the ablation season then further constrain the amount of SWE in the basin. Since ASO is not able to quantify rainfall precipitation, there is additional

uncertainty in the annual water balance that is not reduced by the snow depth updates to the model. However, over the course of the ASO campaign (2013–2018) rain has accounted for approximately only 22% of the total precipitation that has fallen over the Tuolumne (Hedrick et al., 2018). Therefore, the basin remained significantly snow-dominated during the historic drought period and the reduction in snow accumulation and ablation errors using the ASO dataset accounts for the majority of potential SWI input error.

Prior to the first ASO update to the model, P_{SMRF} results in a more topographically complex distribution than P_{PRISM}, yet still a more uniform SWE distribution relative to realistic mountain snowpacks (Figure 2). At the time of the first update, the resulting snow distribution is redefined and SWE is altered throughout the basin. When updates occur after most of the seasonal snow has accumulated, the spatial structure of the ASO-defined distribution is generally maintained by iSnobal throughout the rest of the year, yet still benefits from each subsequent ASO update. For water years 2015 through 2017, iSnobal was run with and without the ASO updates to demonstrate the basin-averaged impact of redefining the snow distribution (Figure 4). An accurate depiction of the SWE spatial distribution allows a more accurate solution to the energy balance model and results in an improved snowpack simulation.

Basin-averaged end of year cumulative SWI in water years 2015 and 2016 was not sensitive to the redistribution of the snowpack from the ASO updates (Figure 4), though it is important to note that the timing of the SWI pulse was advanced by 2–4 weeks during peak streamflow in 2015. The impact of the ASO updates can be seen in the basin averaged SWE from 2015, where the updated spatial distribution caused the snowpack to melt out a full 3 weeks earlier than the modelled SWE without the updates. This is an important result for

water management agencies that rely on exact melt timing for power generation. The insensitivity of the cumulative iSnobal SWI estimates to the updates also indicates that model errors are unbiased.

Water year 2017 was a problematic year for hydrologic modelling in the Tuolumne Basin, primarily due to a lack of precipitation station data at the upper elevations of the catchment. The downscaled HRRR distribution approach described in Section 3.2 and Havens et al. (2019) more accurately captured the large Atmospheric River (AR) events that occurred in January and February of that year, relative to station measurements alone, due to buried/capped precipitation sensors. The first ASO update of 2017 (January 29) decreased SWE by 75 mm (−9%) in the basin (Figure 4), signifying that HRRR had slightly overestimated precipitation mass from the two AR events earlier in January. However, the second update on March 1 added approximately 181 mm (+17%) of SWE storage to the basin. This was because the mass input from the February 7–10 AR event, the same storm which caused the 2017 Oroville Dam spillway disaster in Northern California, was much larger than that predicted by HRRR or captured by station measurements. Lastly, the June 3 update increased SWE storage by 82 mm (+11%), likely due to underestimates in modelled albedo melting snow too quickly throughout the month of May.

4.1 | Closing the water balance

The main goal of this study is to determine how ET and RE are affected by water availability and snow fraction. To achieve this goal, we can use the water balance of the hydrologic inputs and outputs to the Tuolumne Basin through three climatically very dissimilar years (Figure 5). The P_{SMRF} and Q estimates each contain an estimated
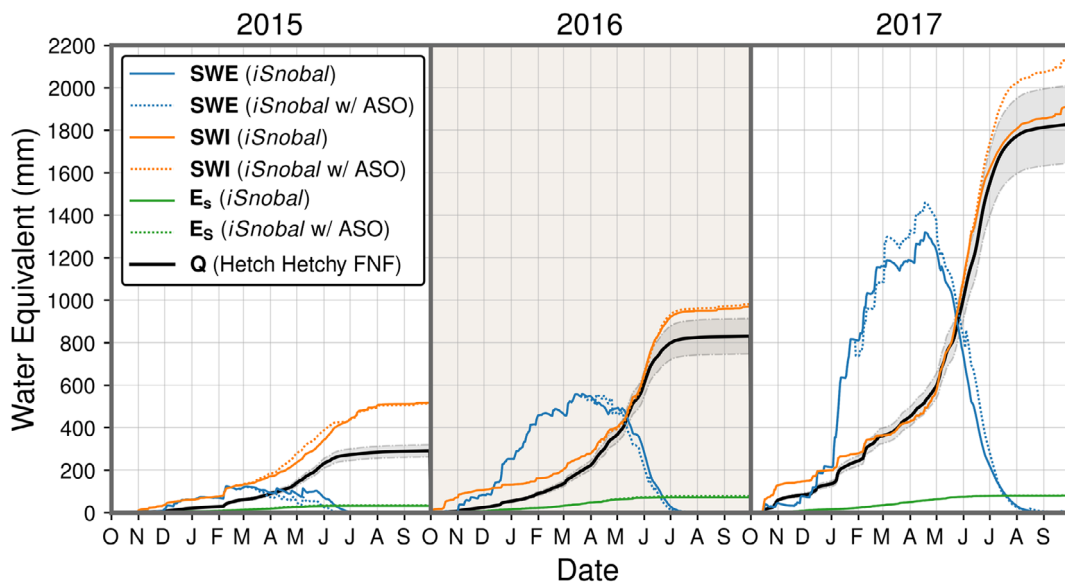

FIGURE 4 Basin-averaged products for the Tuolumne Basin (2015–2017). Solid lines represent iSnobal estimated snow water equivalent (blue), cumulative surface water input (orange), evaporative losses from the snow surface (green), as well as the estimated full natural flow (FNF) at the outlet at Hetch Hetchy Reservoir (black). Dotted lines show the Airborne Snow Observatory-updated iSnobal results for each variable. The grey shaded area is the ±10% uncertainty in the FNF estimates (Lundquist et al., 2016)

±10% error, while the *iSnobal* SWI and E_S estimates were given a ± 3.3% uncertainty following the increased accuracy from the ASO updates (Hedrick et al., 2018).

In annual *iSnobal* simulations without snow depth updates, Equation (4) remains true, and P_{SMRF} = SWI + E_S due to the energy and mass balance nature of the model. To consider the effect of the ASO updates, we introduce a new mass input term, P_{ASO}, that is the sum of the ASO-updated SWI and E_S terms. This pseudo-precipitation term differs from P_{SMRF} because each update changes the overall SWE storage in the basin and reduces uncertainty in the annual precipitation estimate due to the reduced uncertainty in the ASO-updated SWI and E_S model products. In 2015 and 2016, the SMRF and ASO updated precipitation difference ($P_{SMRF} - P_{ASO}$) was only 3 and −19 mm, respectively, yet was much more substantial at −205 mm in 2017 (Figure 5), highlighting a possible underestimation of input precipitation from the HRRR forecast model. More years of analysis are required to determine if the HRRR precipitation in the Tuolumne is always biased low, or if the cause of the underestimated precipitation in 2017 was due to the sheer number of large storms that year.

By using the assumptions described in Section 3, we determine the overall annual evaporative loss terms, ET_{SMRF} and ET_{ASO}, by differencing Q from P_{SMRF} and P_{ASO}, respectively. These evaporative terms contain all loss terms resulting from evaporation/sublimation from the snow surface, evaporation of water after snowmelt and prior to reservoir inflow, and plant transpiration throughout the catchment. Propagating the uncertainty shows that ET_{SMRF} and ET_{ASO} are relatively similar in 2015 and 2016 but differ significantly in 2017 since

the ASO updates in 2017 effectively added 205 mm of precipitation to the basin in the form of additional SWE. Also, the updates resulted in P_{ASO} (2,211 mm) being much closer to P_{PRISM} (2,295 mm) than P_{SMRF} (2,006 mm) in that year.

We then define ET_{WB} as the ASO-updated water balance-derived ET with the *iSnobal*-modelled atmospheric losses from the snow surface removed ($ET_{WB} = ET_{ASO} - E_S$). We use this approach for comparison, because most conventional satellite and model products mask ET estimates when the ground is snow-covered. For the three water years of this study ET_{WB} ranged from 222 ± 34 mm in 2015 to 151 ± 89 mm in 2016 and to 299 ± 196 mm in 2017. Uncertainty increased in each successive year because precipitation, which increased each year, is the largest source of uncertainty in this water-balance approach. Additionally, as mentioned in Section 3.5, the preceding California drought could have drawn down the aquifer causing $\Delta S > 0$ mm and thus ET_{WB} to be overestimated in the following years of increased precipitation input. However, annual ET_{WB} values for 2015–2017 are similar to other previous studies in the region by Henn, Newman, et al. (2018), Fellows and Goulden (2017), and Leydecker and Melack (2000). The following section will address the validation of ET_{WB} using an independent satellite-derived product.

4.2 | Evapotranspiration comparison

The MOD16 Global Product was masked to cells within the Tuolumne Basin to produce cumulative and 8-day ET (ET_{MOD}) and PET (PET_{MOD})
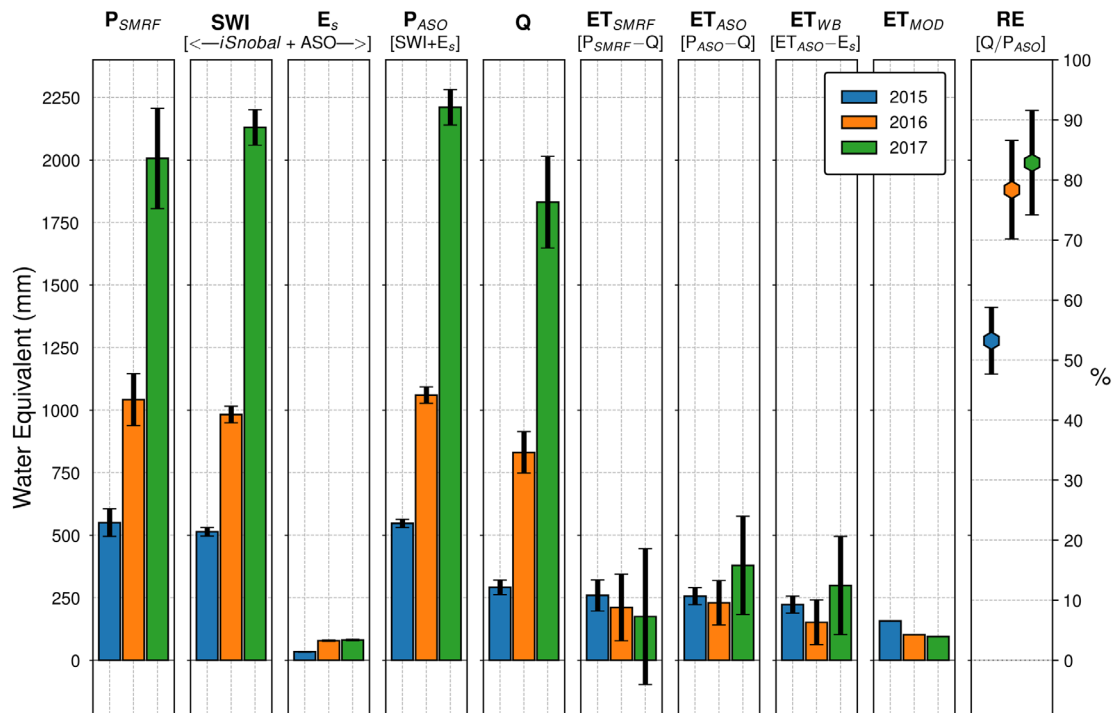

FIGURE 5 Cumulative annual hydrologic inputs and outputs for 2015–2017 in the Tuolumne Basin with associated uncertainty bounds. At the present time, there is no estimate of uncertainty on the ET_{MOD} term from the MOD16 satellite product. Also, annual runoff efficiency is plotted as a percent on the far right

totals (Figure 6). Even though this derived satellite product is corrected for occlusion by snow, cloud, cloud shadow, and bare ground surfaces, the effect of snowpack persistence can be observed in the data. Since complete melt out occurred much earlier in 2015, the MOD16 algorithm predicted a much earlier increase in plant transpiration than in 2016 and 2017. Cumulative ET$_{MOD}$ was 157 mm in 2015, 101 mm in 2016, and just 94 mm in 2017 (Figure 6). Cumulative PET-$_{MOD}$ was 992 mm in the driest year of 2015, 778 mm in the average year of 2016, and 637 mm in the water surplus year of 2017.

The ET$_{MOD}$ cumulative annual totals were lower than estimates of ET put forth by previous studies (Fellows & Goulden, 2017; Henn, Painter, et al., 2018; Kattelmann & Elder, 1991; Leydecker & Melack, 2000). The MOD16 algorithm masks a pixel whenever snow is present, so a certain proportion of actual ET was absent since vegetation often begins to transpire before complete snow melt out, or even remain active throughout the winter at lower elevations albeit at a reduced rate (Trujillo, Molotch, Goulden, Kelly, & Bales, 2012). This explains the large discrepancy between ET$_{WB}$ and ET$_{MOD}$ in 2017 since the melt season in that year was very prolonged due to the larger volume of snow that needed to melt. The length of time after the snowpack became isothermal and the vegetation began transpiring could have been weeks or even months. The fact that the MOD16 ET product and others like it are masked when snow is present likely introduces a low bias in ET estimates for high alpine basins like the Tuolumne. On the other hand, accounting for the transpiration losses during the melt season requires using a water-balance approach with well-quantified precipitation estimates. We note that the assumption that annual $\Delta S \approx 0$ (Equation (3)) affects the determination of ET$_{WB}$. By the end of the 2012–2015 drought period, the deep aquifer was likely drawn down and a portion of the 2017 precipitation could have been lost to deep subsurface recharge that did not end up coming out

of the basin outlet. Not accounting for this loss could have resulted in an overestimation in ET$_{WB}$.

ET$_{MOD}$, like ET$_{WB}$, showed much less variability than total water input (SWI) throughout these 3 years. The low relative variability of these two independent ET estimates among these three dissimilar years might suggest that vegetation growth (i.e., transpiration) in this high elevation basin (above 1,150 m) is less limited by water availability. This would be consistent with previous studies that have shown that forests in the Sierra Nevada become energy-limited above 2,100–2,600 m (Das, Stephenson, Flint, Das, & van Mantgem, 2013; Tague, Heyn, & Christensen, 2009; Trujillo et al., 2012). Since two-thirds of the Tuolumne Basin above Hetch Hetchy lies higher than 2,600 m, the catchment is primarily energy-limited and therefore buffered against drastic swings in short term precipitation variability (<5 years). High elevation annual ET is then possibly balanced by the inverse relationship between seasonal water availability and growing season duration. Lower elevation forests in the region (below 2,100–2,600 m) are water-limited, experience less variable growing season durations from year to year and receive less annual snowfall precipitation. These are likely contributing factors to higher tree mortality (Bales et al., 2018) and greater decreases in ET during droughts found at these elevations.

4.3 | Runoff efficiencies

A hydrologic metric of a basin often used by water managers to describe hydrologic responses to input precipitation is the annual RE, which is defined as the ratio of basin outflow, or reservoir inflow, to basin input precipitation. In the 3 years of this study, the RE (as a percentage) varied from 53 ± 5% in 2015, 78 ± 7% in 2016, and 82 ± 8%
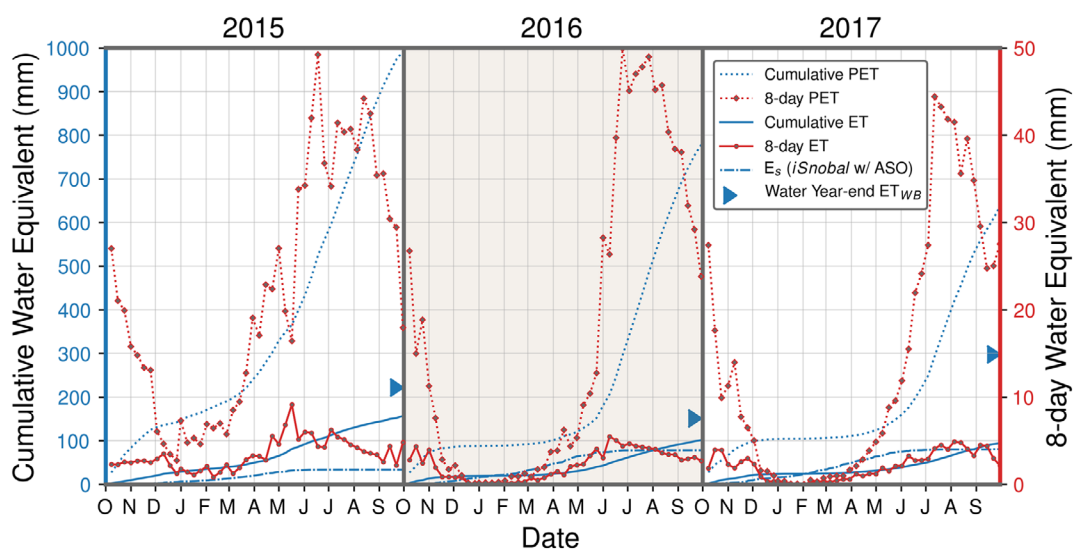

FIGURE 6 Basin-averaged evapotranspiration (ET) and Potential ET losses estimated by the cloud and snow-cover corrected MOD16 gridded 500 m product for water years 2015–2017 over the Tuolumne Basin. The left y-axis and the blue lines represent cumulative totals over each year, while the right y-axis and the red lines are the 8-day sumtotals. Cumulative modelled evaporation and sublimation from the snow surface (E$_S$) and year-end total ET$_{WB}$ are also included for reference
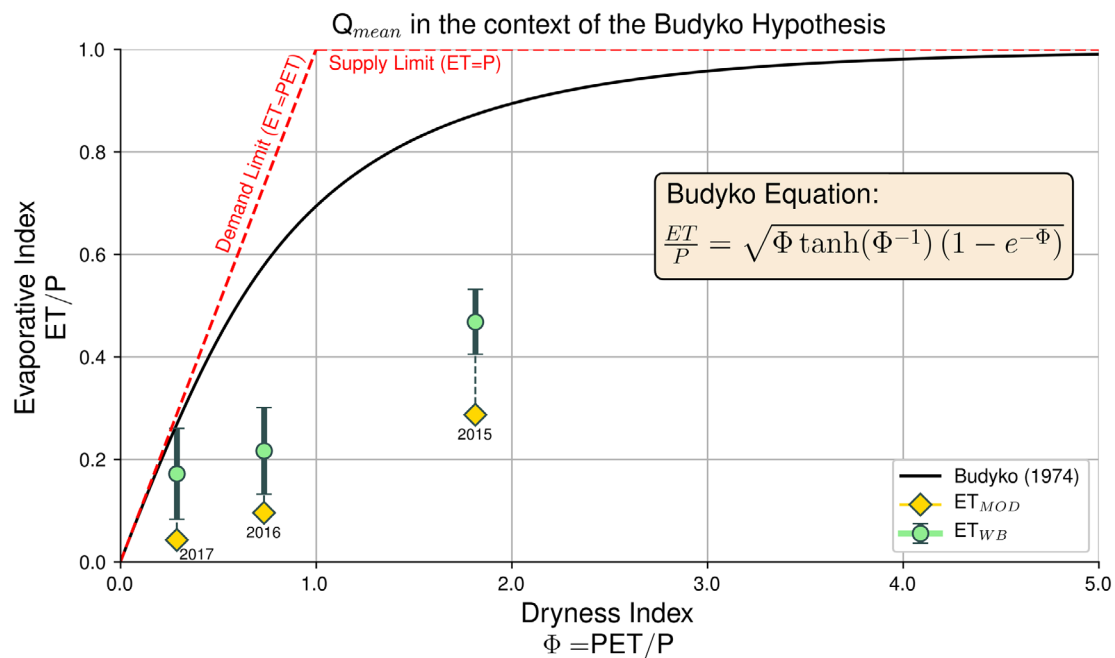
FIGURE 7 Representation of the Tuolumne River Basin annual water balance in the context of the Budyko framework. Potential evapotranspiration (ET) estimates were derived by the MOD16 global ET product (500 m nominal resolution). Two methods of estimating ET are shown: (a) MOD16 global ET (diamonds) and (b) the residual of the water balance with uncertainty included (circles), formulated as the difference between *iSnobal* surface water input and Hetch Hetchy reservoir inflow

in 2017 (Figure 5). These values of RE, especially in 2016 and 2017, are much higher than typical values reported for watersheds in more continental mountain locations and can be traced to the unique lithology of the upper Tuolumne. In fact, extending this water balance approach to estimate ET and RE in other basins may prove difficult due to the assumptions made possible by the granitic geologic makeup of this basin. We attribute the lower RE in 2015 to a combination of (a) increased contribution to the depleted aquifer storage from the previous few years of drought, and (b) increased ET during an extended snow-free season. This assessment is consistent with the findings of Berghuijs et al. (2014), Cooper et al. (2018), and Godsey et al. (2014), who showed that increases in rainfall precipitation proportions across historically snow-dominated basins resulted in lower runoff amounts.

The 2016 average year and 2017 surplus year had similar snow proportions of precipitation (82 and 84%, respectively) as well as RE, with 2017 just receiving significantly more precipitation. However, 2015 had a lower snow proportion of precipitation (70%) to coincide with a much lower RE. Therefore, these results appear to suggest that RE in the Tuolumne Basin is nonlinearly correlated with total annual precipitation and the average snow fraction. Additional water years that were not preceded by historic drought will need to be analysed to determine exactly how this nonlinear relationship is structured and if there are multiyear basin lag times responsible for the apparent changes in RE.

The RE values reported here apply to an entire snow-dominated basin at an annual time scale. RE values pertinent to water managers are dynamic through time and space and depend on factors such as

elevation, vegetation, time of year, and even possibly ecological changes such as forest fire and tree mortality (Biederman et al., 2015). An assessment of sub-annual changes in RE would require an alternate approach since the water balance assumptions detailed in Section 3 do not hold for time periods of less than 1 year.

4.4 | Tuolumne streamflow in the Budyko hypothesis context

Over the last half century, the Budyko Hypothesis (Budyko, 1974) has been applied to dozens of studies on hydrologic supply and demand of water in ostensibly different watersheds. The hypothesis centers on a functional relationship between average annual P and ET over a suitably long period of time. The same assumptions of net zero groundwater storage and aquifer recharge that allow the Budyko Hypothesis to be valid are applied in this study, only here on an annual scale. This approach permits an analysis of how each year varies across a single basin relative to the Budyko functional relationship.

Berghuijs et al. (2014) showed that historically snow-dominated catchments generally have higher runoff efficiencies. Those findings are further corroborated here by plotting the water balance terms of 2015–2017 in Budyko space (Figure 7). We place each year on the plot using the P_{ASO} and ET_{WB} terms from our water balance, in addition to the MOD16 ET and PET products. The ET_{MOD} product was lower than ET_{WB} in all 3 years (Figures 5 and 7). If we assume that ET_{WB} is the "most accurate" estimate of ET over the three study years, it follows that this headwater catchment does not closely

follow the Budyko functional relationship. Thus, the RE of the Tuolumne Basin (RE = 1 – ET/P), as a function of the Dryness Index (PET/P), does not decrease as drastically as predicted by the Budyko hypothesis. The conceptual explanation of this relationship is that the accumulated snowpack acts as a natural surface reservoir that delivers water to the hydrologic system when plant uptake is at its highest level. With future climate scenarios predicting lower snowfall fractions across most mountain watersheds, any previously derived functional relationships between RE and precipitation will be significantly altered.

5 | CONCLUSIONS

This study used a combination of remote sensing and physically based modelling within a snow-dominated basin to examine responses of the hydrologic loss terms of the water balance over varying climatic conditions. Over three markedly dissimilar water years, the residual term in the water balance equation, here representing ET, was determined by accurately accounting for the magnitude and timing of precipitation inputs to the basin. The major conclusions are as follows:

1. Remote sensing-improved estimates of basin precipitation input, in this case represented by modelled daily SWI and E_S, permit a more accurate estimate of the water balance residual than meteorological station data or atmospheric forecast products alone. Under the assumption that subsurface storage flux from year to year is minimal and that the residual value is primarily comprised of evaporative losses to the atmosphere, this subsequently results in a more accurate estimate of ET. If those storage fluxes are positive, as would be the case during aquifer recharge after a drought, then estimates of ET from a water balance perspective would be overestimated.

2. The water balance ET and the satellite-derived ET product varied much less than the input precipitation (P_{ASO}) into the basin over these three years (2015–2017). Even though the 2012–2015 drought likely changed the overall balance of ET, storage flux, and aquifer recharge in the basin, the evaporative losses remained relatively constant regardless of total water availability. However, this conclusion excludes the effects of the preceding drought on the assumption of zero annual subsurface storage flux. Once future additional years of ASO and *iSnobal* become available, a lengthier examination of drought effects on the water balance will be made possible.

3. Basin-averaged annual ET estimates over the three years from the MOD16 satellite-derived product were lower than the existing literature. This satellite product is hampered by snow cover duration, so that estimates of ET are reduced in large snow years when plant transpiration is non-negligible throughout the extended snowmelt period.

4. The annual RE of a watershed is not a static descriptive parameter. Rather, this work shows that RE increases with the total amount of

input precipitation. However, RE in the Tuolumne is affected by the snow fraction of precipitation, as shown by the Budyko analysis. This finding implies that water managers will need to continually consider storm temperature and precipitation phase throughout the year to maintain an idea of how much water will be entering downstream reservoirs. Finally, with future annual temperatures in high mountain basins only expected to rise, we should generally expect decreases in annual RE in coming years.

DATA AVAILABILITY STATEMENT
The ASO snow depth data used to periodically update the snow model are openly available from the National Snow and Ice Data Center at https://nsidc.org/data/ASO_50M_SD/versions/1. Model code for the Spatial Modelling for Resources Framework used to produce iSnobal results is located at https://github.com/USDA-ARS-NWRC/smrf/tree/v0.4.9.

ORCID
Andrew R. Hedrick https://orcid.org/0000-0001-9511-1341

REFERENCES

Bales, R. C., Goulden, M. L., Hunsaker, C. T., Conklin, M. H., Hartsough, P. C., O'Geen, A. T., … Safeeq, M. (2018). Mechanisms controlling the impact of multi-year drought on mountain hydrology. *Scientific Reports*, *8*(1), 690. https://doi.org/10.1038/s41598-017-19007-0

Belmecheri, S., Babst, F., Wahl, E. R., Stahle, D. W., & Trouet, V. (2016). Multi-century evaluation of Sierra Nevada snowpack. *Nature Climate Change*, *6*(1), 2–3. https://doi.org/10.1038/nclimate2809

Benjamin, S. G., Weygandt, S. S., Brown, J. M., Hu, M., Alexander, C. R., Smirnova, T. G., … Manikin, G. S. (2016). A North American hourly

assimilation and model forecast cycle: The rapid refresh. *Monthly Weather Review*, 144(4), 1669–1694. https://doi.org/10.1175/MWR-D-15-0242.1

Berghuijs, W. R., Woods, R. A., & Hrachowitz, M. (2014). A precipitation shift from snow towards rain leads to a decrease in streamflow. *Nature Climate Change*, 4(7), 583–586. https://doi.org/10.1038/NCLIMATE2246

Biederman, J. A., Somor, A. J., Harpold, A. A., Gutmann, E. D., Breshears, D. D., Troch, P. A., ... Brooks, P. D. (2015). Recent tree die-off has little effect on streamflow in contrast to expected increases from historical studies. *Water Resources Research*, 51(12), 9775–9789. https://doi.org/10.1002/2015WR017401

Brutsaert, W. (1982). *Evaporation into the atmosphere: Theory, history, and applications*. Dordrecht, Netherlands: Reidel. http://dx.doi.org/10.1007/978-94-017-1497-6

Budyko, M. I. (1974). In D. H. Miller (Ed.), *Climate and Life*. Orlando, FL: Academic.

Cleugh, H. A., Leuning, R., Mu, Q., & Running, S. W. (2007). Regional evaporation estimates from flux tower and MODIS satellite data. *Remote Sensing of Environment*, 106(3), 285–304. https://doi.org/10.1016/j.rse.2006.07.007

Cooper, M. G., Schaperow, J. R., Cooley, S. W., Alam, S., Smith, L. C., & Lettenmaier, D. P. (2018). Climate elasticity of low flows in the maritime Western U.S. mountains. *Water Resources Research*, 54(8), 5602–5619. https://doi.org/10.1029/2018WR022816

Daly, C., Neilson, R. P., & Phillips, D. L. (1994). A statistical-topographic model for mapping climatological precipitation over mountainous terrain. *Journal of Applied Meteorology*, 33(2), 140–158. https://doi.org/10.1175/1520-0450(1994)033<0140:astmfm>2.0.co;2

Das, A. J., Stephenson, N. L., Flint, A., Das, T., & van Mantgem, P. J. (2013). Climatic correlates of tree mortality in water- and energy-limited forests. *PLoS One*, 8(7), e69917. https://doi.org/10.1371/journal.pone.0069917

Enzminger, T. L., Small, E. E., & Borsa, A. A. (2019). Subsurface water dominates Sierra Nevada seasonal hydrologic storage. *Geophysical Research Letters*, 46(21), 11993–12001. https://doi.org/10.1029/2019GL084589

Feld, S. I., Cristea, N. C., & Lundquist, J. D. (2013). Representing atmospheric moisture content along mountain slopes: Examination using distributed sensors in the Sierra Nevada, California. *Water Resources Research*, 49(7), 4424–4441. https://doi.org/10.1002/wrcr.20318

Fellows, A. W., & Goulden, M. L. (2017). Mapping and understanding dry season soil water drawdown by California montane vegetation. *Ecohydrology*, 10(1), e1772. https://doi.org/10.1002/eco.1772

Garen, D. C., Johnson, G. L., & Hanson, C. L. (1994). Mean areal precipitation for daily hydrologic modelling in mountainous regions. *JAWRA Journal of the American Water Resources Association*, 30(3), 481–491. https://doi.org/10.1111/j.1752-1688.1994.tb03307.x

Garfin, G. M., Gonzalez, P., Breshears, D., Brooks, K., Brown, H. E., Elias, E., ... Udall, B. (2018). Southwest. In *Impacts, risks, and adaptation in the United States: The fourth national climate assessment* (Vol. II). Washington, DC: U.S. Global Change Research Program. https://doi.org/10.7930/NCA4.2018.CH25

Godsey, S. E., Kirchner, J. W., & Tague, C. L. (2014). Effects of changes in winter snowpacks on summer low flows: Case studies in the Sierra Nevada, California, USA. *Hydrological Processes*, 28(19), 5048–5064. https://doi.org/10.1002/hyp.9943

Goulden, M. L., Anderson, R. G., Bales, R. C., Kelly, A. E., Meadows, M., & Winston, G. C. (2012). Evapotranspiration along an elevation gradient in California's Sierra Nevada. *Journal of Geophysical Research: Biogeosciences*, 117(G3), 1–13. https://doi.org/10.1029/2012JG002027

Grünewald, T., Bühler, Y., & Lehning, M. (2014). Elevation dependency of mountain snow depth. *The Cryosphere*, 8(6), 2381–2394. https://doi.org/10.5194/tc-8-2381-2014

Havens, S., Marks, D., FitzGerald, K., Masarik, M., Flores, A. N., Kormos, P., & Hedrick, A. R. (2019). Approximating input data to a snowmelt model using weather research and forecasting model outputs in lieu of meteorological measurements. *Journal of Hydrometeorology*, 20(5), 847–862. https://doi.org/10.1175/JHM-D-18-0146.1

Havens, S., Marks, D., Kormos, P. R., & Hedrick, A. R. (2017). Spatial modelling for resources framework (SMRF): A modular framework for developing spatial forcing data for snow modeling in mountain basins. *Computers & Geosciences*, 109, 295–304. https://doi.org/10.1016/j.cageo.2017.08.016

Hedrick, A. R., Marks, D., Havens, S., Robertson, M., Johnson, M., Sandusky, M., ... Painter, T. H. (2018). Direct insertion of NASA airborne snow observatory-derived snow depth time-series into the *iSnobal* energy balance snow model. *Water Resources Research*, 54, 8045–8063. https://doi.org/10.1029/2018WR023190

Henn, B., Newman, A. J., Livneh, B., Daly, C., & Lundquist, J. D. (2018). An assessment of differences in gridded precipitation datasets in complex terrain. *Journal of Hydrology*, 556, 1205–1219. https://doi.org/10.1016/j.jhydrol.2017.03.008

Henn, B., Painter, T. H., Bormann, K. J., McGurk, B., Flint, A. L., Flint, L. E., ... Lundquist, J. D. (2018). High-elevation evapotranspiration estimates during drought: Using streamflow and NASA airborne snow observatory SWE observations to close the upper Tuolumne River basin water balance. *Water Resources Research*, 54(2), 746–766. https://doi.org/10.1002/2017WR020473

Herrmann, F., Keller, L., Kunkel, R., Vereecken, H., & Wendland, F. (2015). Determination of spatially differentiated water balance components including groundwater recharge on the Federal State level—A case study using the mGROWA model in North Rhine-Westphalia (Germany). *Journal of Hydrology: Regional Studies*, 4, 294–312. https://doi.org/10.1016/j.ejrh.2015.06.018

Jentsch, A., Kreyling, J., & Beierkuhnlein, C. (2007). A new generation climate-change experiments: Events, not trends. *Frontiers in Ecology and the Environment*, 5(7), 365–374.

Kattelmann, R., & Elder, K. J. (1991). Hydrologic characteristics and water balance of an Alpine Basin in the Sierra Nevada. *Water Resources Research*, 27(7), 1553–1562. https://doi.org/10.1029/90WR02771

Kendy, E., Gérard-Marchant, P., Todd Walter, M., Zhang, Y., Liu, C., & Steenhuis, T. S. (2003). A soil-water-balance approach to quantify groundwater recharge from irrigated cropland in the North China plain. *Hydrological Processes*, 17(10), 2011–2031. https://doi.org/10.1002/hyp.1240

Kirchner, P. B., Bales, R. C., Molotch, N. P., Flanagan, J., & Guo, Q. (2014). LiDAR measurement of seasonal snow accumulation along an elevation gradient in the southern Sierra Nevada, California. *Hydrology and Earth System Sciences*, 18(10), 4261–4275. https://doi.org/10.5194/hess-18-4261-2014

Knowles, J. F., Harpold, A. A., Cowie, R., Zeliff, M., Barnard, H. R., Burns, S. P., ... Williams, M. W. (2015). The relative contributions of alpine and subalpine ecosystems to the water balance of a mountainous, headwater catchment. *Hydrological Processes*, 29(22), 4794–4808. https://doi.org/10.1002/hyp.10526

Kormos, P. R., Marks, D., McNamara, J. P., Marshall, H. P., Winstral, A., & Flores, A. N. (2014). Snow distribution, melt and surface water inputs to the soil in the mountain rain–snow transition zone. *Journal of Hydrology*, 519, 190–204. https://doi.org/10.1016/j.jhydrol.2014.06.051

Kunkel, K. E., Robinson, D. A., Champion, S., Yin, X., Estilow, T., & Frankson, R. M. (2016). Trends and extremes in northern hemisphere snow characteristics. *Current Climate Change Reports*, 2(2), 65–73. https://doi.org/10.1007/s40641-016-0036-8

Lehning, M., Grünewald, T., & Schirmer, M. (2011). Mountain snow distribution governed by an altitudinal gradient and terrain roughness. *Geophysical Research Letters*, 38(19), 1–5. https://doi.org/10.1029/2011GL048927

Leydecker, A., & Melack, J. (2000). Estimating evaporation in seasonally snow-covered catchments in the Sierra Nevada, California. *Journal of*

Hydrology, *236*(1-2), 121–138. https://doi.org/10.1016/S0022-1694(00)00290-0

Luce, C. H., Vose, J. M., Pederson, N., Campbell, J., Millar, C., Kormos, P. R., & Woods, R. (2016). Contributing factors for drought in United States forest ecosystems under projected future climates and their uncertainty. *Forest Ecology and Management*, *380*, 299–308. https://doi.org/10.1016/j.foreco.2016.05.020

Lundquist, J. D., Dettinger, M. D., & Cayan, D. R. (2005). Snow-fed streamflow timing at different basin scales: Case study of the Tuolumne River above Hetch Hetchy, Yosemite, California. *Water Resources Research*, *41*(7), 1–14. https://doi.org/10.1029/2004WR003933

Lundquist, J. D., Roche, J. W., Forrester, H., Moore, C., Keenan, E., Perry, G., ... Dettinger, M. D. (2016). Yosemite hydroclimate network: Distributed stream and atmospheric data for the Tuolumne River watershed and surroundings. *Water Resources Research*, *52*(9), 7478–7489. https://doi.org/10.1002/2016WR019261

Marks, D., Domingo, J., Susong, D., Link, T., & Garen, D. (1999). A spatially distributed energy balance snowmelt model for application in mountain basins. *Hydrological Processes*, *13*(12-13), 1935–1959. https://doi.org/10.1002/(SICI)1099-1085(199909)13:12/13<1935::AID-HYP868>3.0.CO;2-C

Marks, D., & Dozier, J. (1992). Climate and energy exchange at the snow surface in the alpine region of the Sierra Nevada: 2. Snow cover energy balance. *Water Resources Research*, *28*(11), 3043–3054. https://doi.org/10.1029/92WR01483

Marks, D., Kimball, J., Tingey, D., & Link, T. (1998). The sensitivity of snowmelt processes to climate conditions and forest cover during rain-on-snow: A case study of the 1996 Pacific Northwest flood. *Hydrological Processes*, *12*(10-11), 1569–1587. https://doi.org/10.1002/(SICI)1099-1085(199808/09)12:10/11<1569::AID-HYP682>3.0.CO;2-L

Marks, D., Winstral, A. H., Flerchinger, G. N., Reba, M. L., Pomeroy, J. W., Link, T. E., & Elder, K. J. (2008). Comparing simulated and measured sensible and latent heat fluxes over snow under a pine canopy to improve an energy balance snowmelt model. *Journal of Hydrometeorology*, *9*(6), 1506–1522. https://doi.org/10.1175/2008JHM874.1

May, C., Luce, C. H., Casola, J. H., Chang, M., Cuhaciyan, J., Dalton, M., ... York, E. A. (2018). Northwest. In *Impacts, risks, and adaptation in the United States: The fourth national climate assessment* (Vol. II). Washington, DC: U.S. Global Change Research Program. https://doi.org/10.7930/NCA4.2018.CH24

Mu, Q., Heinsch, F. A., Zhao, M., & Running, S. W. (2007). Development of a global evapotranspiration algorithm based on MODIS and global meteorology data. *Remote Sensing of Environment*, *111*(4), 519–536. https://doi.org/10.1016/j.rse.2007.04.015

Mu, Q., Zhao, M., & Running, S. W. (2011). Improvements to a MODIS global terrestrial evapotranspiration algorithm. *Remote Sensing of Environment*, *115*(8), 1781–1800. https://doi.org/10.1016/j.rse.2011.02.019

Musselman, K., Pomeroy, J., Essery, R., & Leroux, N. (2015). Impact of windflow calculations on simulations of alpine snow accumulation, redistribution and ablation. *Hydrological Processes*, *29*(18), 3983–3999. https://doi.org/10.1002/hyp.10595

Painter, T. H. (2018). ASO L4 Lidar snow depth 3m UTM grid, version 1. Boulder, Colorado, USA: NASA National Snow and Ice Data Center Distributed Active Archive Center. https://doi.org/10.5067/KIE9QNVG7HP0

Painter, T. H., Berisford, D. F., Boardman, J. W., Bormann, K. J., Deems, J. S., Gehrke, F., ... Winstral, A. (2016). The airborne snow observatory: Fusion of scanning Lidar, imaging spectrometer, and physically-based modeling for mapping snow water equivalent and snow albedo. *Remote Sensing of Environment*, *184*, 139–152. https://doi.org/10.1016/j.rse.2016.06.018

Pomeroy, J., Gray, D. M., & Landine, P. G. (1993). The prairie blowing snow model: Characteristics, validation, operation. *Journal of Hydrology*, *144*(1-4), 165–192. https://doi.org/10.1016/0022-1694(93)90171-5

Raleigh, M. S., & Small, E. E. (2017). Snowpack density modeling is the primary source of uncertainty when mapping basin-wide SWE with Lidar. *Geophysical Research Letters*, *44*(8), 3700–3709. https://doi.org/10.1002/2016GL071999

Rasmussen, R., Baker, B., Kochendorfer, J., Meyers, T., Landolt, S., Fischer, A. P., ... Gutmann, E. (2012). How well are we measuring snow: The NOAA/FAA/NCAR winter precipitation test bed. *Bulletin of the American Meteorological Society*, *93*(6), 811–829. https://doi.org/10.1175/BAMS-D-11-00052.1

Reba, M. L., Marks, D., Winstral, A., Link, T. E., & Kumar, M. (2011). Sensitivity of the snowcover energetics in a mountain basin to variations in climate. *Hydrological Processes*, *25*(21), 3312–3321. https://doi.org/10.1002/hyp.8155

Rice, R., Bales, R. C., Painter, T. H., & Dozier, J. (2011). Snow water equivalent along elevation gradients in the Merced and Tuolumne River basins of the Sierra Nevada. *Water Resources Research*, *47*(8), 1–11. https://doi.org/10.1029/2010WR009278

Roche, J. W., Goulden, M. L., & Bales, R. C. (2018). Estimating evapotranspiration change due to forest treatment and fire at the basin scale in the Sierra Nevada, California. *Ecohydrology*, *11*, e1978. https://doi.org/10.1002/eco.1978

Roderick, M. L., Sun, F., Lim, W. H., & Farquhar, G. D. (2014). A general framework for understanding the response of the water cycle to global warming over land and ocean. *Hydrology and Earth System Sciences*, *18*(5), 1575–1589. https://doi.org/10.5194/hess-18-1575-2014

Roe, G. H., & Baker, M. B. (2006). Microphysical and geometrical controls on the pattern of orographic precipitation. *Journal of the Atmospheric Sciences*, *63*(3), 861–880. https://doi.org/10.1175/JAS3619.1

Running, S. W., Mu, Q., & Zhao, M. (2017). MOD16A2 MODIS/Terra net evapotranspiration 8-day L4 global 500m SIN grid V006 [data set]. NASA EOSDIS Land Processes DAAC. https://doi.org/10.5067/MODIS/MOD16A2.006

Seager, R., Naik, N., & Vogel, L. (2012). Does global warming cause intensified interannual hydroclimate variability? *Journal of Climate*, *25*(9), 3355–3372. https://doi.org/10.1175/JCLI-D-11-00363.1

Sohrabi, M. M., Tonina, D., Benjankar, R., Kumar, M., Kormos, P., Marks, D., & Luce, C. (2019). On the role of spatial resolution on snow estimates using a process-based snow model across a range of climatology and elevation. *Hydrological Processes*, *33*, 1260–1275. https://doi.org/10.1002/hyp.13397

Stern, M. A., Anderson, F. A., Flint, L. E., & Flint, A. L. (2018). Soil moisture datasets at five sites in the central Sierra Nevada and northern Coast Ranges, California: U.S. Geological Survey Data Series 1083. https://doi.org/10.3133/ds1083

Tague, C., Heyn, K., & Christensen, L. (2009). Topographic controls on spatial patterns of conifer transpiration and net primary productivity under climate warming in mountain ecosystems. *Ecohydrology*, *2*(4), 541–554. https://doi.org/10.1002/eco.88

Trujillo, E., Molotch, N. P., Goulden, M. L., Kelly, A. E., & Bales, R. C. (2012). Elevation-dependent influence of snow accumulation on forest greening. *Nature Geoscience*, *5*(10), 705–709. https://doi.org/10.1038/ngeo1571

Trujillo, E., Ramírez, J. A., & Elder, K. J. (2007). Topographic, meteorologic, and canopy controls on the scaling characteristics of the spatial distribution of snow depth fields. *Water Resources Research*, *43*(7), 1–17. https://doi.org/10.1029/2006WR005317

Trujillo, E., Ramírez, J. A., & Elder, K. J. (2009). Scaling properties and spatial organization of snow depth fields in sub-alpine forest and alpine tundra. *Hydrological Processes*, *23*, 1575–1590. https://doi.org/10.1002/hyp.7270

Viviroli, D., Dürr, H. H., Messerli, B., Meybeck, M., & Weingartner, R. (2007). Mountains of the world, water towers for humanity: Typology, mapping, and global significance. *Water Resources Research*, *43*(7), 1–13. https://doi.org/10.1029/2006WR005653

Wan, Z., Zhang, K., Xue, X., Hong, Z., Hong, Y., & Gourley, J. J. (2015). Water balance-based actual evapotranspiration reconstruction from ground and satellite observations over the conterminous United States. *Water Resources Research*, *51*(8), 6485–6499. https://doi.org/10.1002/2015WR017311

Williams, C. A., Reichstein, M., Buchmann, N., Baldocchi, D., Beer, C., Schwalm, C., ... Schaefer, K. (2012). Climate and vegetation controls on the surface water balance: Synthesis of evapotranspiration measured across a global network of flux towers. *Water Resources Research*, *48*(6), 1–13. https://doi.org/10.1029/2011WR011586

Winstral, A. H., Marks, D., & Gurney, R. (2013). Simulating wind-affected snow accumulations at catchment to basin scales. *Advances in Water Resources*, *55*, 64–79. https://doi.org/10.1016/j.advwatres.2012.08.011